Nanoscale Horizons

COMMUNICATION

Check for updates

Phosphinecarboxamide based InZnP QDs – an air tolerant route to luminescent III–V semiconductors†

Yi Wang,[a] Jack Howley,[b] Erica N. Faria,[b] Chen Huang,[cd] Sadie Carter-Searjeant,[a] Simon Fairclough,[e] Angus Kirkland,[cd] Jason J. Davis, [iD][g] Falak Naz,[f] Muhammad Tariq Sajjad, [iD][f] Jose M. Goicoechea*[h] and Mark Green [iD]*[a]

We describe a new synthetic methodology for the preparation of high quality, emission tuneable InP-based quantum dots (QDs) using a solid, air- and moisture-tolerant primary phosphine as a group-V precursor. This presents a significantly simpler synthetic pathway compared to the state-of-the-art precursors currently employed in phosphide quantum dot synthesis which are volatile, dangerous and air-sensitive, *e.g.* $P(Si(CH_3)_3)_3$.

The advent of modern quantum dots (QD) as technologically relevant materials can be traced back to 1993, when a landmark paper married organometallic chemistry and high temperature, inert atmosphere, solution-based synthesis, resulting in II–VI nanomaterials of a previously unobtainable quality.[1] The success of this route can be directly related to the reagents employed, specifically developed as solution analogues of vapour phase precursors for high quality semiconducting materials. Whilst the group II elements were initially supplied *via* a metal alkyl, Steigerwald's 'masked atom' approach to group VI elements using alkylphosphine chalcogenides can be seen as a pioneering step that made chalcogenides routinely available in organic solvent-based, high temperature nanoparticle

New concepts

Quantum dots (QDs) are ubiquitous and are now considered a well-developed technology, although most are based on a toxic metal system – cadmium selenide. The obvious replacement is indium phosphide, however, the synthetic chemistry in the synthesis of InP based QDs has barely developed in over three decades since 1989, and uses the highly reactive, dangerous, volatile, air-sensitive phosphorous precursor tris(trimethylsilyl)phosphine. In our report, we describe the use of an air tolerant, solid phosphorous precursor that is relatively simple and safe to use, allowing manipulations of the precursors in ambient conditions on the bench prior to QD synthesis. The resulting QDs are emission tuneable, brightly emitting and this synthetic development can fit directly into existing QD chemistry notably in the manufacture of engineered core/shell architectures. This greatly improves the ease of QD synthesis, both in the lab and potentially in industry.

synthesis.[2] However, cadmium chalcogenide QDs are unlikely to be widely adopted due to recent regulations and general concerns regarding the use of toxic metals.[3]

Group III–V semiconducting compounds (notably InP) provide an attractive alternative to cadmium-based nanomaterials, with recent studies describing InP-based QD with optical properties comparable to their II–VI analogues.[4] However, the basic synthetic chemistry remains essentially unchanged for over 30 years. In landmark reports, the dehalosilylation reaction, first reported by Healy *et al.*[5] and by Wells *et al.*[6] in 1989 described solution routes to III–V materials exploiting the volatile, highly pyrophoric and reactive liquids $E(Si(CH_3)_3)_3$ (E = P, As) as solution equivalents to phosphine or arsine gas (PH_3 or AsH_3). This precursor chemistry was developed for the preparation of III–V QDs by Mićić *et al.*[7] and Olshavsky *et al.*[8] and has since been globally adopted. Whilst other precursor routes based on alternative phosphorous delivery methods do exist, the majority are unlikely to find routine application as they are equally difficult and problematic. The use of aminophosphines is notable yet presents only a marginal

a Department of Physics, King's College London, The Strand, London, WC2R 2LS, UK. E-mail: mark.a.green@kcl.ac.uk

b Department of Chemistry, Chemistry Research Laboratory, University of Oxford, Mansfield Road, Oxford, OX1 3TA, UK

c Department of Materials, University of Oxford, Parks Road, Oxford, OX1 3PH, UK

d Electron Physical Sciences Imaging Centre, Diamond Light Source, Harwell Science Innovation Campus. Fermi Ave, Didcot, OX110DE, UK

e Department of Materials Science and Metallurgy, University of Cambridge, 27 Charles Babbage Road, Cambridge, CB3 0FS, UK

f London Centre for Energy Engineering (LCEE), School of Engineering, London South Bank University, 103 Borough Road, London, SE1 0AA, UK

g Physical and Theoretical Chemistry Laboratory, South Parks Road, Oxford, OX1 3QZ, UK

h Department of Chemistry, Indiana University, 800 E. Kirkwood Ave., Bloomington, IN, 47405, USA. E-mail: jgoicoec@iu.edu

† Electronic supplementary information (ESI) available. See DOI: https://doi.org/10.1039/d3nh00162h

improvement, as these similarly volatile liquids yield complicated phosphorous products under thermolysis,[9] whilst the oxides of aminophosphines have been shown to be toxic.[10] In addition, common reagents such as $P(Si(CH_3)_3)_3$ have been shown to be excessively reactive, making it difficult to separate nucleation and focused growth steps. For these reasons, a stable reagent with a well-defined decomposition point that provides the volatile intermediate should allow discrete controlled nucleation not normally afforded by $P(Si(CH_3)_3)_3$.[11,12] To date, the lack of an obvious, well-defined and convenient group V precursor has limited the expansion of III–V based QD relative to their II–VI analogues.

Recently, sodium phosphaethynolate has been used as a new phosphorus precursor to InP quantum dots.[13] NaPCO is not pyrophoric and may be handled under ambient conditions for several hours before decomposing, making it attractive compared to traditional precursors. Phosphinecarboxamide, $PH_2C(O)NH_2$,[14] is readily derived from NaPCO by reaction with ammonium tetrafluoroborate in liquid ammonia and has the advantage of being a metal-free precursor. Phosphinecarboxamide has been used as a phosphorus precursor for the chemical vapor deposition (CVD) of zinc phosphide thin films.[15] It was suggested that upon heating, phosphinecarboxamide decomposed to form PH_3 (alongside isocyanic acid, HNCO), which then reacted with zinc salts to form zinc phosphide. This 'masked' PH_3 reactivity is particularly relevant for III–V QD synthesis, as PH_3 is a known phosphorus precursor to InP. Li et al. showed that by acidification of Ca_3P_2 with HCl, the gaseous PH_3 generated can be reacted with indium salts in solution to form InP QDs.[16] We postulated that if 'masked' PH_3

reactivity could be reproduced in the solution phase, then phosphinecarboxamide should act as a suitable phosphorus source for InP QD synthesis.

We first explored the thermal decomposition of phosphinecarboxamide in solution by ^{31}P NMR spectroscopy. Upon heating at 105 °C, decomposition was evidenced by a decrease in intensity of the characteristic $^{31}P\{^1H\}$ signal at −134.9 ppm (Fig. 1a). The decomposition of PCA also gave rise to two new signals at −212.2 ppm and −240.8 ppm, which may be unambiguously assigned to P_2H_4 and PH_3, respectively, from the proton-coupled spectrum (Fig. 1b). Further evidence of the in situ generation of PH_3 was the formation of characteristic signals of InP clusters by $^{31}P\{^1H\}$ NMR upon reaction with indium phenylacetate at 110 °C (−180 ppm to −250 ppm) (ESI,† Fig. S1). These magic-sized clusters (MSCs), such as $In_{37}P_{20}(COOPh)_{51}$ reported by Cossairt and co-workers, are well characterised intermediates in QD growth.[17] More recently, Zn-alloyed InP MSCs have been elucidated by Kwon et al.[18] The formation of InP clusters from phosphinecarboxamide was also characterized by UV-Vis spectroscopy, where a broad absorption shoulder was observed at ca. 410 nm (ESI,† Fig. S2).

It is worth noting at this stage that upon heating phosphinecarboxamide generates the PH_3 which is in the desired oxidation state of −3, unlike the thermal decomposition products of $P(N(CH_3)_2)_3$, a common precursor, which generates both +3 and −3 species.[9] In this case, the comparison with TOPSe as a precursor falls short, as TOPSe arguably generates selenium in the Se(0) state – in fact, delivery of the reactive intermediate in the correct oxidation state is a key requirement, so the chemistry described here is perhaps more useful. When
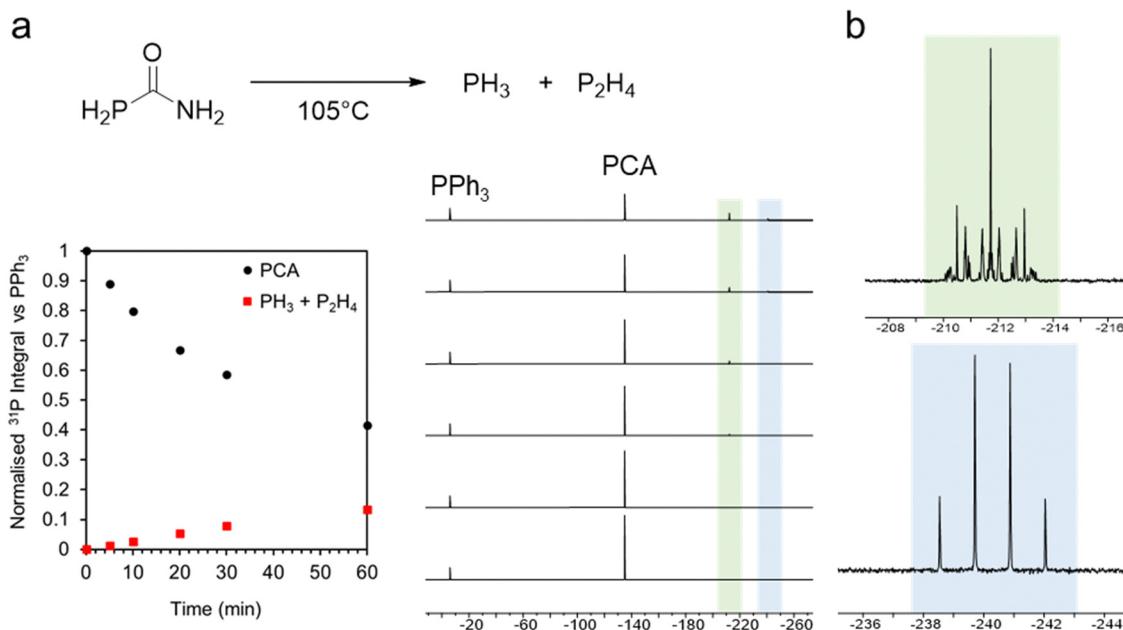

Fig. 1 (a) Thermal decomposition of $PH_2C(O)NH_2$ followed by $^{31}P\{^1H\}$ NMR spectroscopy; (b) ^{31}P NMR spectra of phosphorus–containing decomposition products PH_3 (green) and P_2H_4 (blue).

approaching precursor delivery from this angle, our route might be considered the equivalent of the thiourea/selenourea precursor chemistry described by Owen.[19,20]

These solution-based decomposition studies suggest that phosphinecarboxamide, $PH_2C(O)NH_2$, can act as an effective phosphide precursor. The compound is a solid, air- and moisture-tolerant primary phosphine that can be handled under ambient conditions (and stored indefinitely under an inert atmosphere), making routine handling simple and significantly safer than $P(Si(CH_3)_3)_3$.

A typical reaction is described in the ESI.† In our standard hot solution synthetic route (using the ''heat-up'' method), the resulting nascent phosphine precursors reacted with the *in situ* metal salts ultimately resulting in InZnP QD which exhibited optical properties consistent with InZnP-based QD prepared by other synthetic techniques.

The reaction described here proceeded in two phases, with an initial degassing step of between 30 min and 60 minutes at 120 °C. This initial step had two functions, initially removing dissolved gasses and water, whilst initiating the *in situ* gradual

release of the phosphine precursors. This allowed an unusual method of tuning the resulting QD size by regulating the amount of precursor available. Extended degassing of up to 60 minutes removed a large amount of precursor, resulting in less available precursor and hence the formation of smaller particles with a larger blue shift in the optical band gap and emission spectra. A shorter degassing step resulted in more precursor available for reaction and hence yielded larger particles with optical properties towards the red end of the visible spectrum. Prolonged degassing over 120 minutes resulted in all phosphorus precursor being removed and the reaction failing. This degassing step was followed by a higher temperature growth and annealing for 10 minutes at 220 °C. Further addition (and the subsequent heating) of zinc diethyldithiocarbamate to the resultant core InZnP QD yielded InZnP/ZnS core/shell QD.

The optical properties of the resulting QD were consistent with InP-based nanomaterials with tuneable visible emission observed between the green and red regions of the visible spectrum when excited at 365 nm (Fig. 2). Absorption band
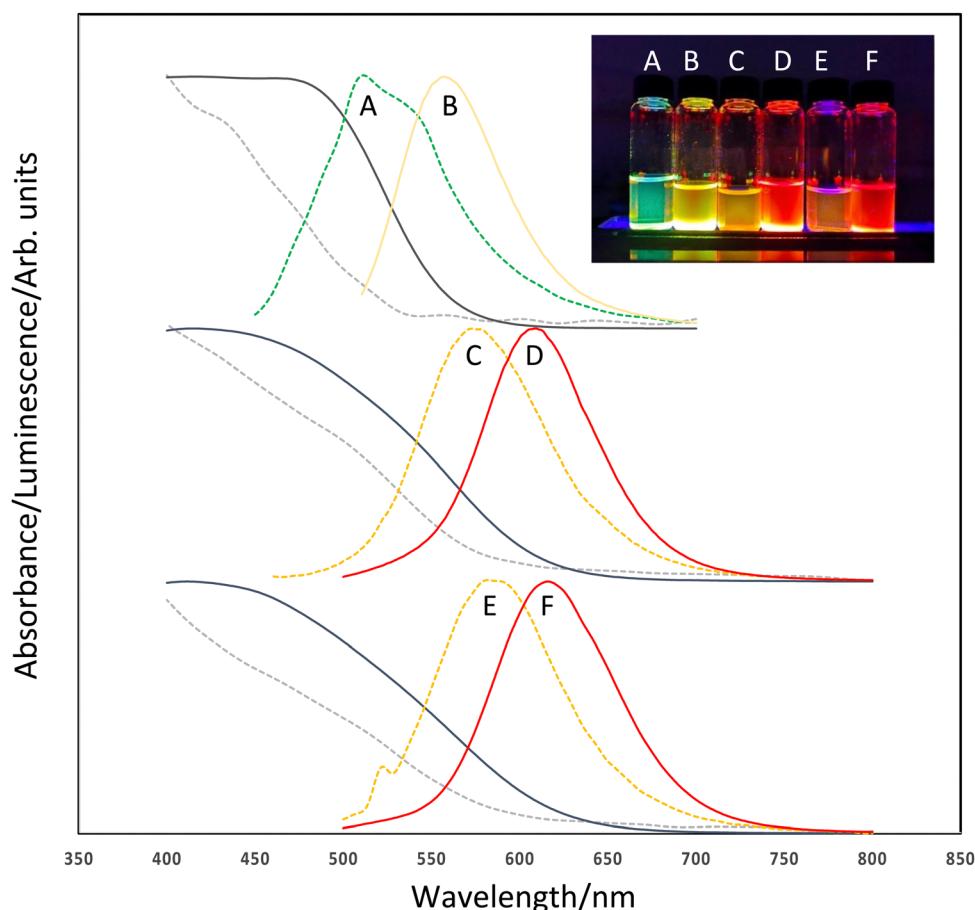
Fig. 2 Emission and absorption spectra of InZnP (dotted lines) and InZnP/ZnS (solid lines) quantum dots. (A) InZnP, degassed for 60 minutes at 120 °C followed by 10 minutes growth at 220 °C. (B) InZnP/ZnS using sample A, with shell growth at 300 °C for 30 minutes. (C) InZnP, degassed for 45 minutes at 120 °C followed by 10 minutes growth at 220 °C. (D) InZnP/ZnS using sample C, with shell growth at 300 °C for 30 minutes. (E) InZnP, degassed at 30 minutes at 120 °C followed by 10 minutes growth at 220 °C. (F) InZnP/ZnS using sample E, with shell grown at 300 °C for 30 minutes. Inset, The range of InZnP and InZnP/ZnS quantum dots in toluene, excited at 365 nm. Unusual features in emission spectra A and E have been assigned as either a second distinct particle size, or surface trap emission.

edges were tuneable and measured between *ca.* 500 nm (InZnP, grown at 60 minutes/120 °C degassing followed by 10 minutes/ 220 °C growth) and *ca.* 600 nm (InZnP/ZnS, core grown at 30 minutes degassing/120 °C followed by 10 minutes/220 °C growth, followed by shell addition) as shown in Fig. 2. It was observed that addition of a ZnS shell resulted in a red shift in the absorption edge from the core particle due to a leak of the exciton into the shell. The emission spectra were tuneable between *ca.* 510 nm (InZnP, 60 minutes/120 °C degassing followed by 10 minutes/220 °C growth) and *ca.* 620 nm (InZnP/ZnS, core grown at 30 minutes/120 °C degassing followed by 10 minutes/220 °C growth, followed by shell addition). The appearance of a second feature in spectrum 2a could either be a second distinct particle size, or surface trap emission. (Likewise, in spectrum 2e, a small artefact from the excitation can be seen at *ca.* 520 nm). The origins of band edge emission in InP based quantum is non-trivial, and emission reported from early example of InP quantum dots often showed unusual features.[21]

The emission FWHM (full width at half the maximum) was found to be between *ca.* 60 and 80 nm, although no attempt was made to narrow this by size fractionation or controlling particle growth. The origin of the broad emission profile has been discussed in a detailed study by Janke *et al.*, highlighting the role of lattice disorder and defects at the III–V/II–VI interface.[22] Similarly, emission quantum yields were *ca.* 4% for the InZnP core only and *ca.* 36% for shelled materials. Emission lifetimes were found to be *ca.* 78 to 83 ns for InZnP particles and *ca.* 65 ns for InZnP/ZnS particles.

Scanning transmission electron microscopy (STEM) of unshelled particles (InZnP, grown at 45 minutes/120 °C degassing followed by 10 minutes/220 °C growth) showed typical images associated with nanoscale InZnP, with small, discrete, slightly anisotropic particles *ca.* 3.0 ± 0.1 nm in diameter, as shown in Fig. 3a. Elemental analysis (ESI,† Fig. S3) confirmed the presence of In, Zn, P, C and O; carbon being attributed to the decomposed capping ligand (hexadecylamine) whilst the oxygen being assigned to a surface oxide species. Previous work

has highlighted that the zinc component is likely to be on or near the surface.[23]

High angle annular dark field (HAADF) scanning transmission electron microscope images of QD of InZnP/ZnS (InZnP/ZnS, core grown at 45 minutes/120 °C degassing followed by 10 minutes/220 °C growth, followed by shell addition at 30 minutes/300 °C) showed larger particles as expected, *ca.* 3.9 ± 0.2 nm in diameter with clearly visible lattice fringes (Fig. 3b and c). The structural nature and identity of InP-based core/shell materials is still unresolved and has been discussed elsewhere. For the current study, InZnP/ZnS is the most appropriate nomenclature although this may be updated in future work.[24] Elemental analysis again confirmed the presence of In, Zn, P, C, O and sulfur (S), as shown in ESI,† Fig. S4, attributed to the ZnS shell which was estimated at approximately 1.45 monolayers thick. The lattice was measured as 0.346 ± 0.01 nm, representative of the [111] plane of zinc blende cubic ZnS, as observed in Fig. 3c. Particle size distribution histograms are supplied in ESI,† Fig. S5. The surface of the quantum dots was not explored in this initial study. X-ray powder diffraction (XRD) shows reflections typical for zinc blende structured InP-based QD with broad, weak reflections that became more pronounced after shell deposition. Specifically, the (111), (220) and (311) reflections were observed for the InZnP/ZnS core/shell materials (InZnP/ZnS, core grown at 30 minutes/120 °C degassing followed by 10 minutes/220 °C growth, followed by shell addition, ESI,† Fig. S6). The intense reflection component at *ca.* 20 2ø has recently been attributed to ordered surface ligands.[25]

The use of a solid, air-tolerant phosphorous precursor makes InP QD significantly easier to prepare, and such an approach might be considered the functional equivalent of trioctylphosphine selenide (TOPSe) acting as a convenient selenium source, as both precursors are relatively stable at room temperature yet act as an efficient precursor source when heated. Whilst detailed studies have uncovered complex reaction mechanisms for the preparation of Cd and Pb-based QDs using trialkylphosphine chalcogenides,[26,27] the rationale for
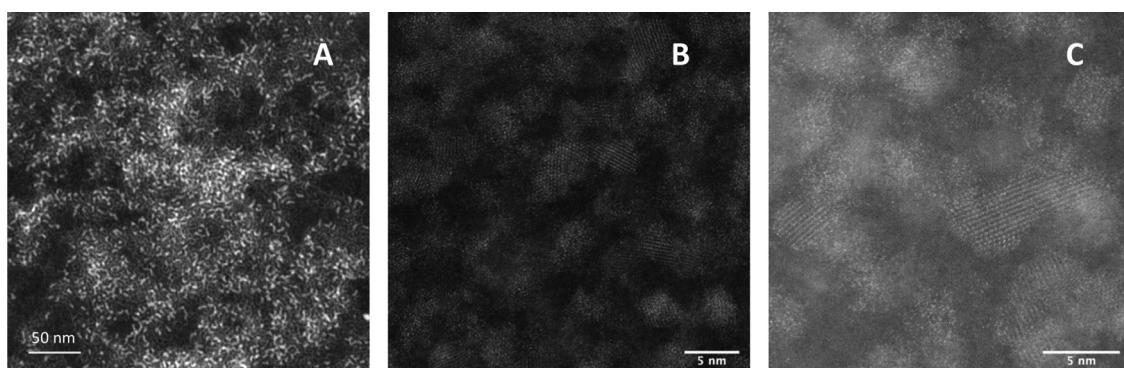
Fig. 3 STEM HAADF image of (A) InZnP (InZnP, grown at 45 minutes/120 °C degassing followed by 10 minutes/220 °C growth). (B), (C) High angle annular dark field (HAADF) STEM images of InZnP/ZnS (InZnP/ZnS, core grown at 45 minutes/120 °C degassing followed by 10 minutes/220 °C growth, followed by shell addition).

our study remains identical – a stable compound which provides a convenient, controllable route to a hitherto relatively inaccessible element/precursor when required in solution semiconductor synthesis.

Phosphinecarboxamide is unusually an air- and moisture-tolerant primary phosphine, which we have shown decomposes to phosphine and diphosphane. The relatively rare stability of primary phosphines is assigned to either steric factors, or the electronic structure which can be engineered, by, for example, the inclusion of heteroatoms that shift the HOMO. The energy of the singly occupied molecular orbital (SOMO) of radical cations has been shown to be a relevant indicator of stability, with a suggested threshold of −10 eV being the criterion.[28] It is worth noting that PCA is not entirely stable and will slowly decompose under ambient conditions over an extended period. Since steric factors are clearly not relevant, the extended stability of PCA has been attributed by Jupp partly to resonance stabilisation of the phosphorus lone pair by the adjacent amide moiety.[29]

In conclusion, we describe the use of a simple, air and moisture tolerant primary phosphine as a convenient precursor for indium phosphide-based QD. The resulting zinc blende crystalline nanomaterials had optical properties which could be tuned through the green/red range of the visible spectrum. This pathway presents a shift in synthetic methodology away from volatile phosphorous compounds towards engineered stable, solid precursors which remain inert until desired in the specific reaction. This precursor route highlights the suitability of specific simple phosphines as convenient precursors towards high quality semiconducting nanomaterials.

Conflicts of interest

There are no conflicts to declare.

Acknowledgements

References

1 C. B. Murray, D. J. Norris and M. G. Bawendi, Synthesis and characterization of nearly monodisperse CdE (E = S, Se, Te) semiconductor nanocrystallites, *J. Am. Chem. Soc.*, 1993, **115**, 8706–8715.

2 S. M. Stuczynski, Y.-U. Kwon and M. L. Steigerwald, The use of phosphine chalcogenides in the preparation of cobalt chalcogenides, *J. Organomet. Chem.*, 1993, **449**, 167–172.

3 M. S. Giroux, Z. Zahra, O. A. Salawu, R. M. Burgess, K. T. Ho and A. S. Adeleye, Assessing the enviornmental effects related to quantum dot structure, function, synthesis and exposure, *Environ. Sci.: Nano*, 2022, **9**, 867–910.

4 S. Tamang, C. Lincheneau, Y. Hermans, S. Jeong and P. Reiss, Chemistry of InP nanocrystal syntheses, *Chem. Mater.*, 2016, **28**, 2491–2506.

5 M. D. Healy, P. E. Laibinis, P. D. Stupik and A. R. Barron, The reaction of indium(III) chloride with tris(trimethylsilyl)phosphine: a novel route to indium phosphide, *Chem. Commun.*, 1989, 359–360.

6 R. L. Wells, C. G. Pitt, A. T. McPhail, A. P. Purdy, S. Shafieezad and R. B. Hallcock, The use of tris(trimethylsilyl)arsine to prepare gallium arsenide and indium arsenide, *Chem. Mater.*, 1989, **1**, 4–6.

7 O. I. Mićić, C. J. Curtis, K. M. Jones, J. R. Sprague and A. J. Nozik, Synthesis and characterization of InP quantum dots, *J. Phys. Chem.*, 1994, **98**, 4966–4969.

8 M. A. Olshavsky, A. N. Goldstein and A. P. Alivisatos, Organometallic synthesis of gallium-arsenide crystallites, exhibiting quantum confinement, *J. Am. Chem. Soc.*, 1990, **112**, 9438–9439.

9 M. D. Tessier, K. De Nolf, D. Dupont, D. Sinnaeve, J. De Roo and Z. Hens, Aminophosphines: a double role in the synthesis of colloidal indium phosphide quantum dots, *Chem. Mater.*, 2016, **138**, 5923–5929.

10 R. Kimbrough and T. B. Gaines, Toxicity of hexamethylphosphoramide in rats, *Nature*, 1966, **211**, 146–147.

11 H. B. Chandrasiri, E. Byoel Kim and P. T. Snee, Sterically encumbered tris(trialkylsilyl)phosphine precursors for quantum dot synthesis, *Inorg. Chem.*, 2020, **59**, 15928–15935.

12 D. C. Gary, B. A. Glassy and B. M. Cossairt, Investigation of indium phosphide quantum dot nucleation and growth utilizing triarylsilylphosphine precursors, *Chem. Mater.*, 2014, **26**, 1734–1744.

13 P. Yu, Y. Shan, S. Cao, Y. Hu, Q. Li, R. Zeng, B. Zou, Y. Wang and J. Zhao, Inorganic solid phosphorus precursor of sodium phosphaethynolate for synthesis of highly luminescent InP-based quantum dots, *ACS Energy Lett.*, 2021, **6**, 2697–2703.

14 A. R. Jupp and J. M. Goicoechea, Phosphinecarboxamide: A Phosphorus-Containing Analogue of Urea and Stable Primary Phosphine, *J. Am. Chem. Soc.*, 2013, **135**, 19131–19134.

15 S. V. F. Beddoe, S. D. Cosham, A. N. Kulak, A. R. Jupp, J. M. Goicoechea and G. Hyett, Phosphinecarboxamide as an unexpected phosphorus precursor in the chemical vapour deposition of zinc phosphide thin films, *Dalton Trans.*, 2018, **47**, 9221–9225.

16 L. Li, M. Protière and P. Reiss, Economic Synthesis of High Quality InP Nanocrystals Using Calcium Phosphide as the Phosphorus Precursor, *Chem. Mater.*, 2008, **20**, 2621–2623.

17 M. R. Friedfeld, D. A. Johnson and B. M. Cossairt, Conversion of InP clusters to quantum dots, *Inorg. Chem.*, 2019, **58**, 803–810.

18 Y. Kwon, J. Oh, E. Lee, S. H. Lee, A. Agnes, G. Bang, J. Kim, D. Kim and S. Kim, Evolution from unimolecular to colloidal-quantum dot-like character in chlorine or zinc

incorporated InP magic size clusters, *Nat. Commun.*, 2020, **11**, 3127.

19 M. P. Campos, M. P. Hendricks, A. N. Beecher, W. Walravens, R. A. Swain, G. T. Cleveland, Z. Hens, M. Y. Sfeir and J. S. Owen, A library of selenourea precursors to PbSe nanocrystals with size distributions near the homogenous limit, *J. Am. Chem. Soc.*, 2017, **139**, 2296–2305.

20 M. P. Hendricks, M. P. Campos, G. T. Cleveland, I. Jen-La Plante and J. S. Owen, A tuneable library of substituted thiourea precursors to metal sulfide nanocrystals, *Science*, 2015, **348**, 1226–1230.

21 O. I. Mićić, C. J. Curtis, K. M. Jones, J. R. Sprague and A. J. Nozik, *J. Phys. Chem.*, 1994, **98**, 4966–4969.

22 E. M. Janke, N. E. Williams, C. She, D. Zherebetskyy, M. H. Hudson, L. Wang, D. J. Gosztola, R. D. Schaller, B. Lee, C. Sun, G. S. Engel and D. V. Talapin, Origin of broad emission spectra in InP quantum dots: contributions from structural and electronic disorder, *J. Am. Chem. Soc.*, 2018, **140**, 15791–15803.

23 N. Kirkwood, A. De Backer, T. Altantzis, N. Winckelmans, A. Longo, F. V. Antolinez, F. T. Rabouw, L. De Trizio, J. J. Geuchies, J. T. Mulder, N. Renaud, S. Bals, L. Manna and A. J. Houtepen, Locating and controlling the Zn content in In(Zn)P quantum dots, *Chem. Mater.*, 2020, **32**, 557–565.

24 M. Burkitt-Gray, M. Casavola, P. C. J. Clark, S. M. Fairclough, W. R. Flavell, R. Fleck, S. J. Haigh, J. Chun-Ren, M. Leontiadou, E. A. Lewsi, J. Osiecki, B. Qazi-Chaudhry, G. Vizcay-Barrena, W. Wichiansee and M. Green, Structural investigatins into colour tuneable fluorescent InZnP-based quantum dots from zinc carboxylate and aminophosphine precursors, *Nanoscale*, 2023, **15**, 1763–1774.

25 J. J. Calvin, T. M. Kaufman, A. B. Sedlak, M. F. Crook and A. P. Alivisatos, Observation of ordered organic capping ligands on semiconducting quantum dots via powder X-ray diffraction, *Nat. Commun.*, 2021, **12**, 2663.

26 H. Liu, J. S. Owen and A. P. Alivisatos, mechanistic study of precursor evolution in colloidal II–VI semiconductor nanocrystal synthesis, *J. Am. Chem. Soc.*, 2007, **129**, 305–312.

27 J. S. Steckel, B. K. H. Yen, D. C. Oertel and M. G. Bawendi, On the mechanism of lead chalcogenide nanocrystal formation, *J. Am. Chem. Soc.*, 2006, **128**, 13032–13033.

28 B. Stewart, A. Harriman and L. J. Higham, Predicting the air stability of phosphines, *Organometallics*, 2011, **30**, 5338–5343.

29 A. R. Jupp, *D.Phil. thesis*, University of Oxford, 2016.